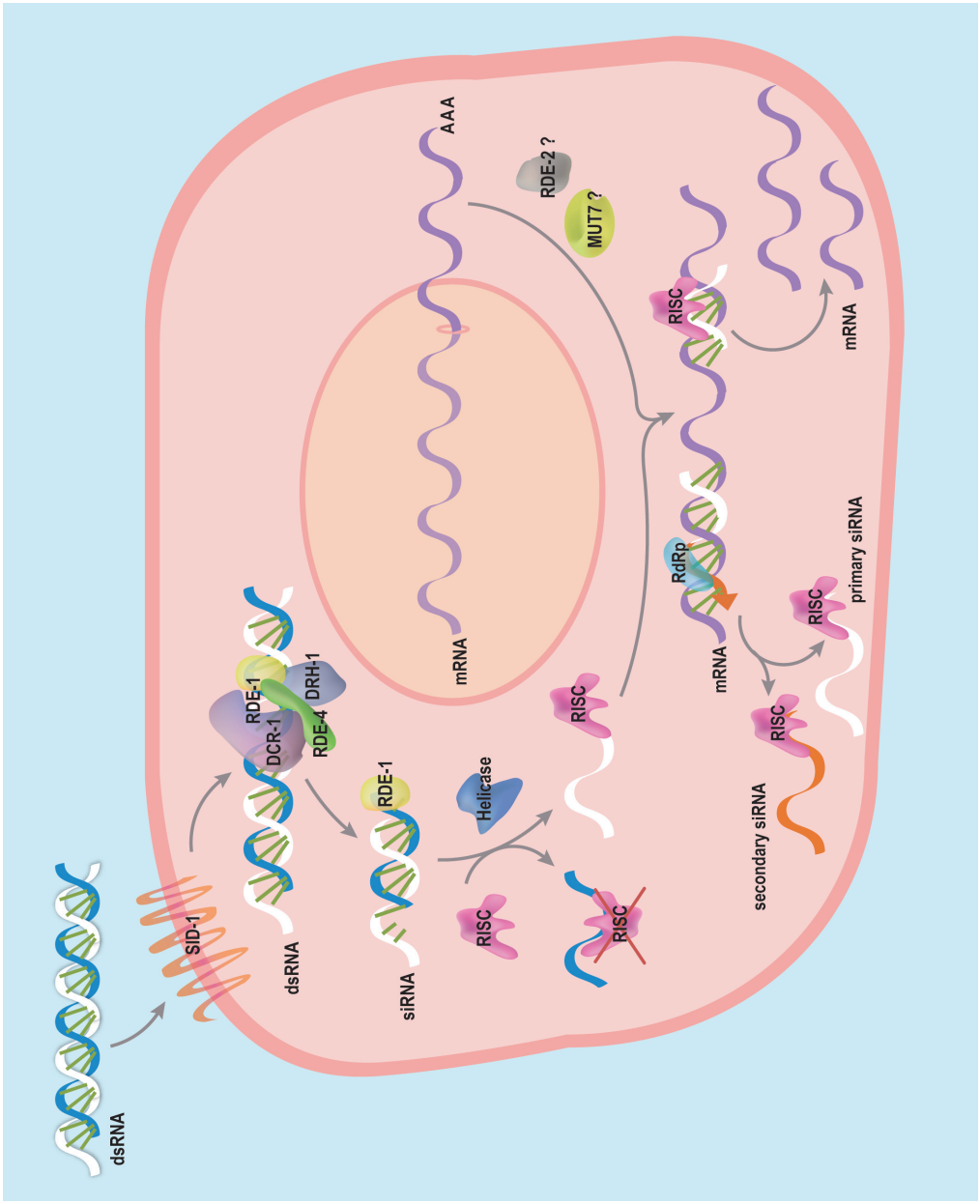

Figure 1.1. Model of RNAi pathway in *C. elegans*. Transmembrane protein SID-1 allows dsRNA to enter the cell. In the cytoplasm, dsRNA gets processed by DCR-1, existing in a complex with RDE-4, RDE-1 and DRH-1. The resulting siRNA is shown bound to RDE-1. Double stranded siRNA is unwound by a helicase, allowing RISC complex to bind single strands of siRNA. RDE-2 and MUT-7 might help in bringing together target mRNA and antisense siRNA (white) bound to RISC. RISC, guided by siRNA (white), degrades mRNA. Antisense siRNA also serves as a primer for RdRp, which uses mRNA as a template and produces more antisense siRNAs (orange). Sense siRNAs (blue) do not accumulate in *C. elegans*.

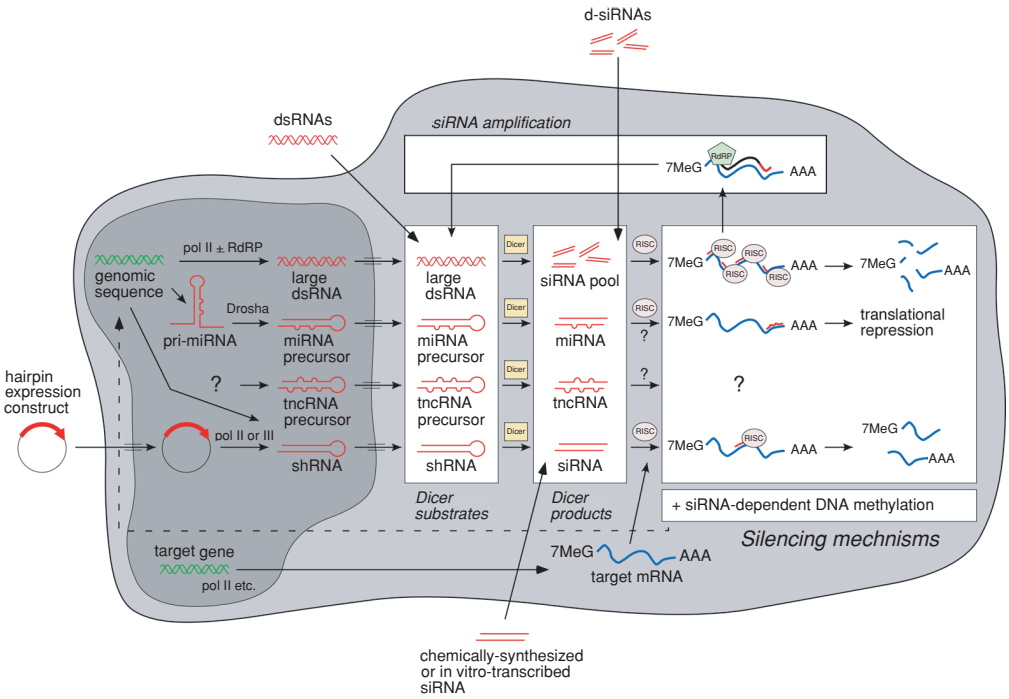

Figure 2.1. Sequence dependent regulation of gene expression. Expression of particular genomic sequences produces various dsRNAs. Dicer is responsible for processing the dsRNAs into small RNAs. The small RNA is then incorporated into RISC, guiding the protein complex to a specific mRNA. RISC enforces specific gene suppression either by cleavage of the mRNA or inhibition of translation. The degree of complementarity between the small RNA and the mRNA determines the fate of the mRNA; perfect or near perfect complementarity generally results in cleavage of the mRNA, whereas, a few mismatches results in suppression of translation. In a sequence specific manner, small RNAs also regulate chromatin structure and hence gene expression. Some of the processes depicted here may not be present in all organisms or cell types. From a practical standpoint small RNAs can be used to investigate gene function; several types of small dsRNAs can either be introduced into the cell or produced inside the cell. In all cases the small RNA is funneled into the RNAi pathway and triggers specific gene suppression.

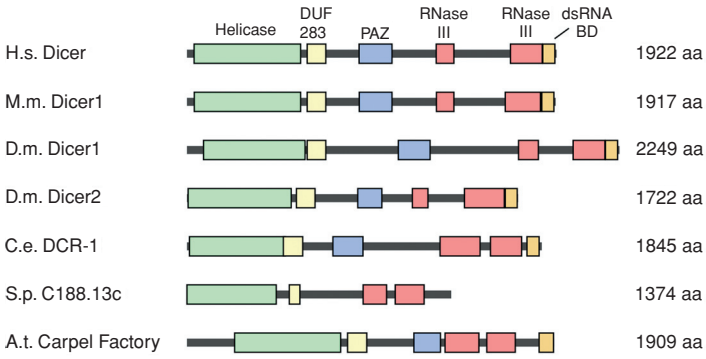

Figure 2.2. Alignment of Dicer homologs. Most Dicer proteins contain six conserved domains: a DExH helicase domain; a domain of unknown function (DUF283); a PAZ domain; two RNase III catalytic domains; and finally a double stranded RNA binding domain. Spacing between the domains is different for the homologs, which may explain the different size classes of small RNAs found in some species.

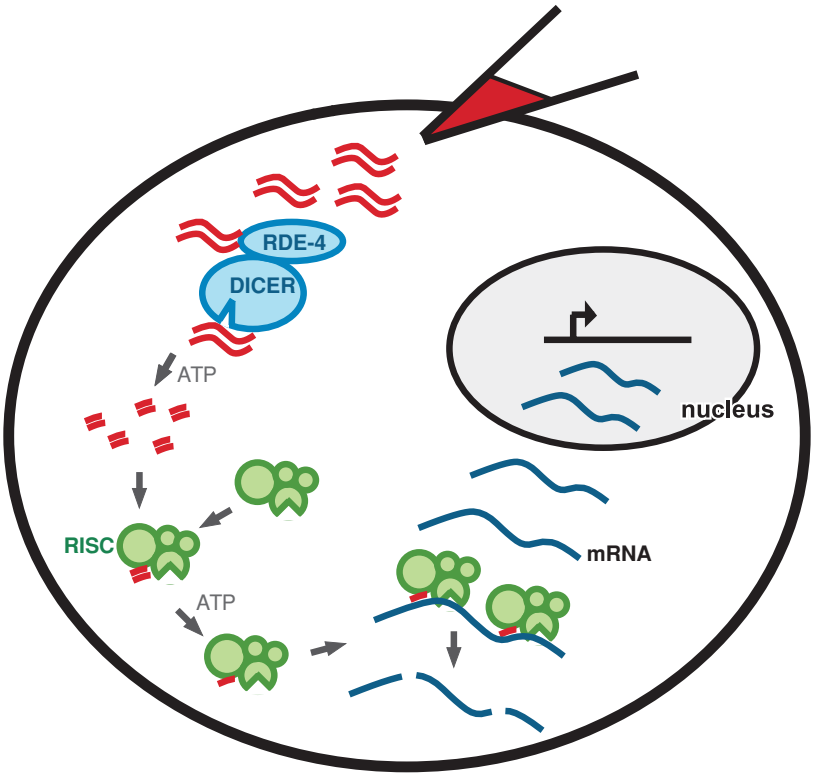

Figure 3.1. Model for mRNA degradation in the cytoplasm by RNAi. Introduced dsRNAs (red) are recognized by RDE-4/R2D2, a dsRNA binding protein. These dsRNAs are then processed by Dicer into 21-23nt duplexes that can associate with an enzyme complex called RISC. After unwinding of the siRNAs, RISC becomes competent to target homologous mRNA transcripts for degradation.

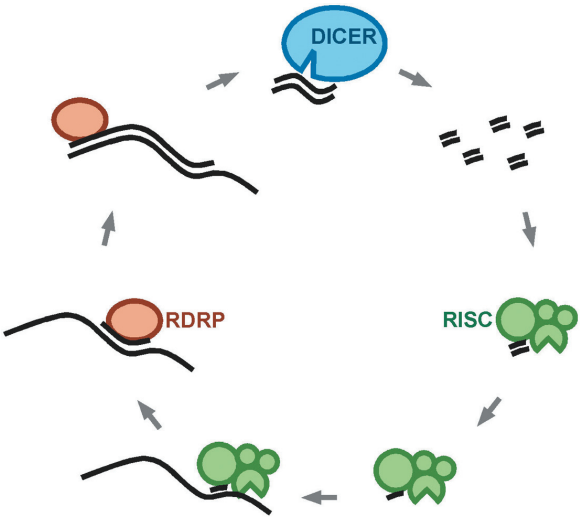

Figure 3.2. Amplification of dsRNA by an RNA-dependent RNA polymerase. In certain organisms, new dsRNAs can be generated by RDRPs, primed by siRNAs on mRNA targets. The new dsRNAs can be used subsequently by Dicer to create more siRNAs, which can lead to additional rounds of amplification.

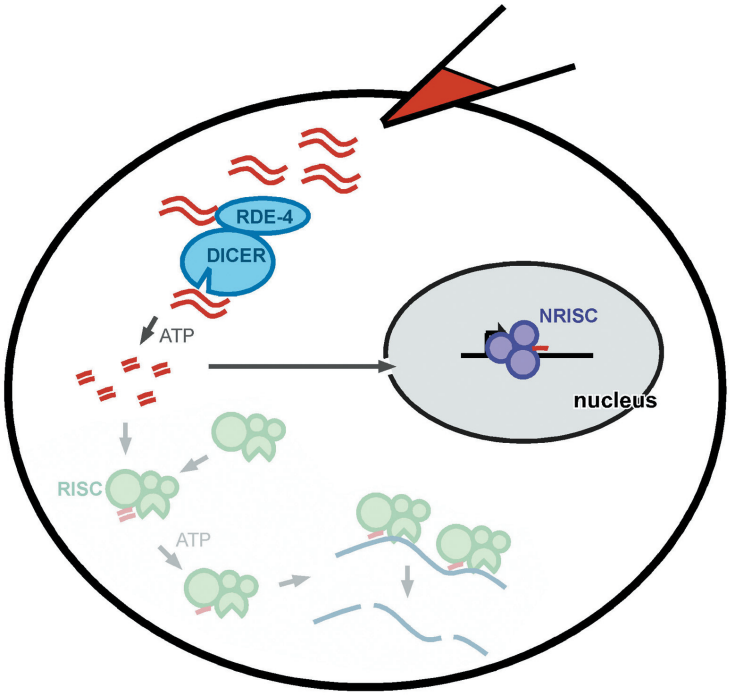

Figure 3.3. Model for gene silencing in the nucleus by RNAi. RNAi can also silence the transcription of targeted genes in certain organisms. In this model a signal can direct a putative nuclear RNAi silencing complex (NRISC), composed of chromatin modifying proteins, to the targeted locus, silencing gene expression at the level of transcription.

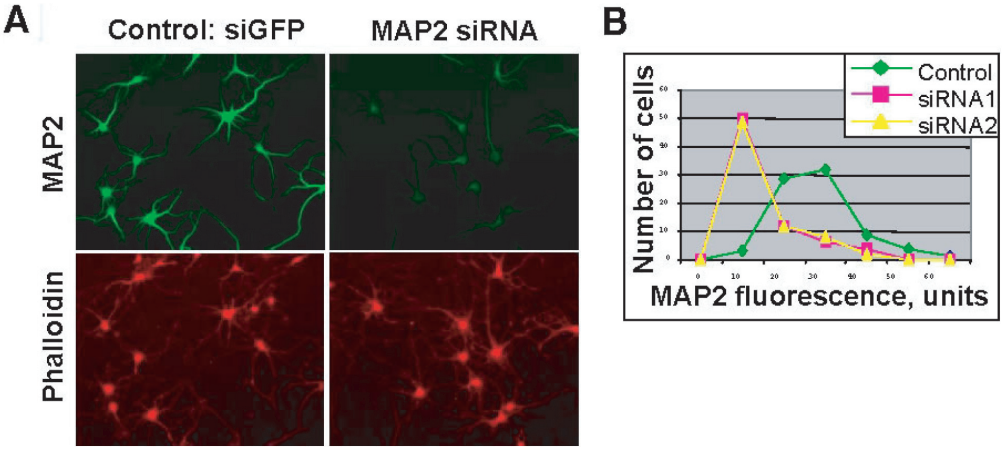

Figure 5.4. Microtubule Associated Protein 2 (MAP2) suppression in primary cortical neurons by cognate 21nt-siRNAs. A. Double fluorescence staining of neurons transfected with non-specific siRNA or with MAP2-siRNA. Upper panels-staining with MAP2 monoclonal antibody (green); lower panels-staining with actin-bound toxin phalloidin (red). B. Distribution of MAP2 expression levels in control and targeted cells, two different siRNA (siRNA1 and siRNA2) show a very similar effect. In each experiment, at least 70 random neurons per experimental condition were analyzed and gene expression was quantified in both control and targeted cells. The figure is reprinted from: Krichevsky, A. M. and Kosik, K. S. "RNAi functions in cultured mammalian neurons." *Proc Natl Acad Sci U S A.*, **99**(18):11926–9 (2002).

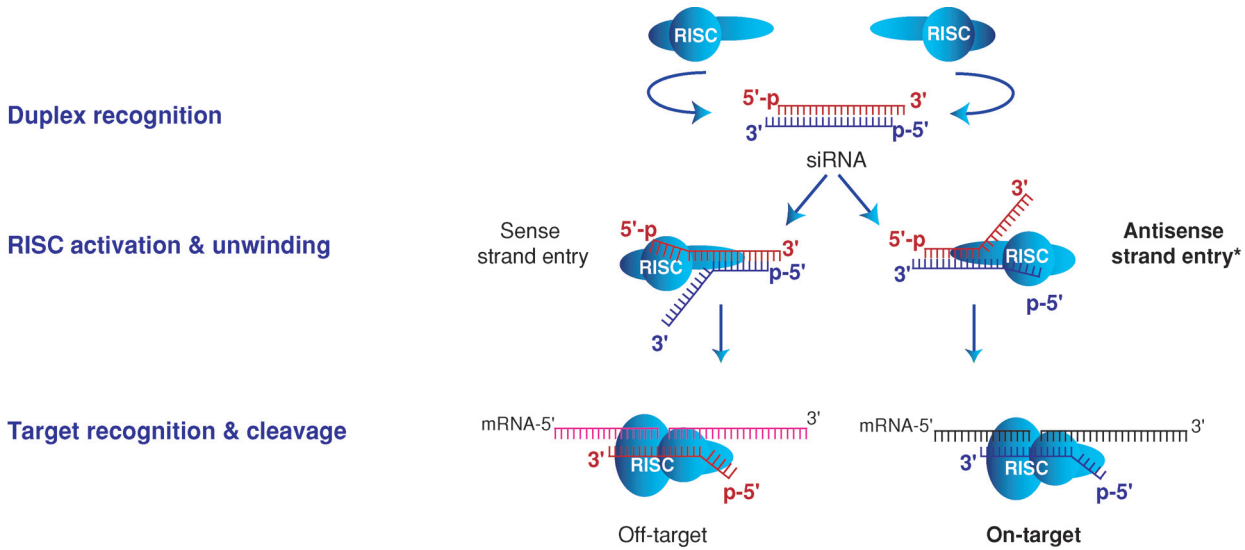

Figure 6.2. A model for the siRNA-mediated RNAi mechanism depicting major steps in (1) initial duplex recognition by the pre-RISC complex; (2) ATP-dependent RISC activation and siRNA unwinding, (3) target recognition, (4) target cleavage and product release. The desired outcome is directed by antisense strand entry* into the RISC to produce "on-target" silencing effects. Undesirable off-target effects are thought to be directed by sense strand identity to unrelated sequences but can be minimized using rational design coupled with comprehensive sequence analyses.

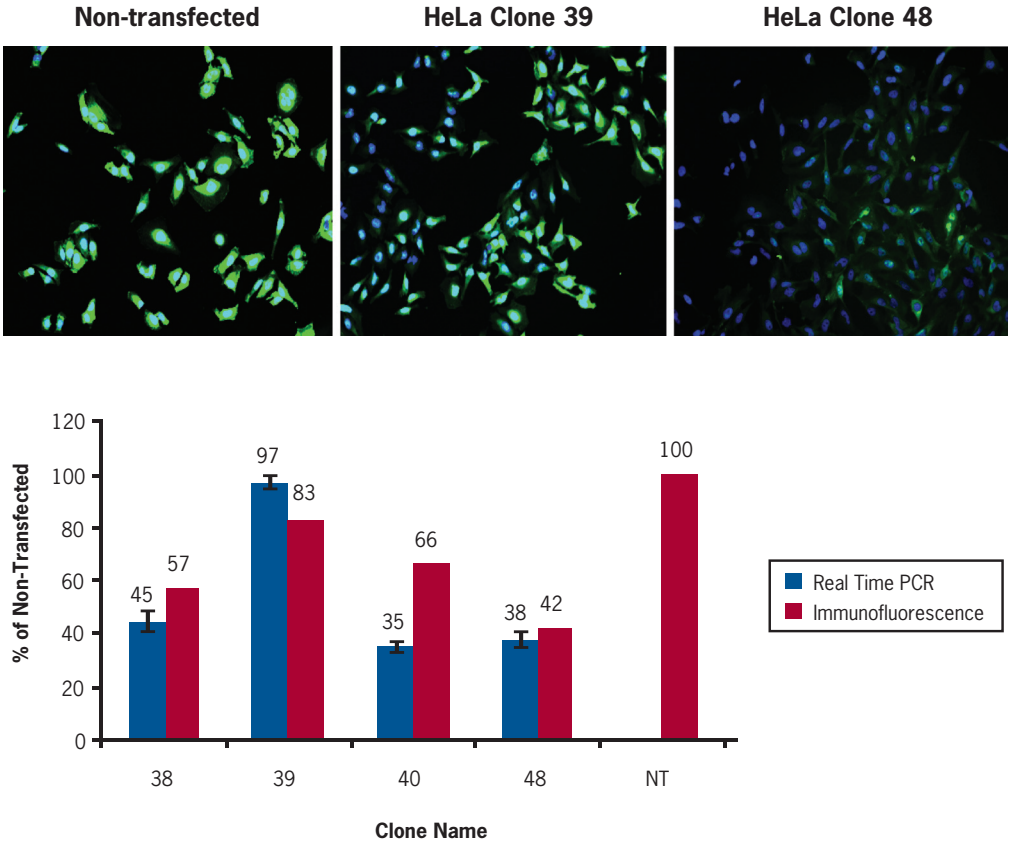

Figure 10.3. Long Term Silencing of GAPDH with CMV Puro Plasmid. HeLa cells were transfected with a CMV puro plasmid expressing GAPDH-specific siRNAs. The cells were cloned, and clonal populations were selected in 2.5 μg/ml puromycin. Three weeks after selection, GAPDH expression was analyzed by (A) RT-PCR or (B) immunofluorescence. Expression levels of several cell clones are shown. Green: GAPDH. Blue: DAPI stained nuclei.

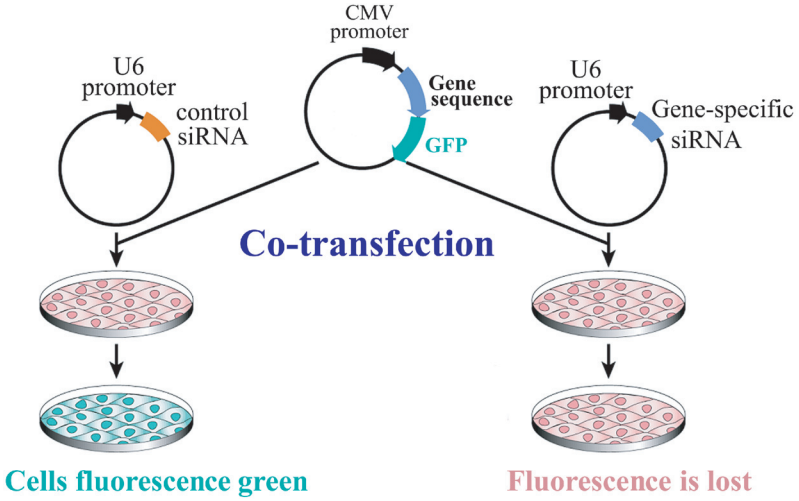

Figure 11.4. Method for identifying effective shRNA sequences. To screen for siRNAs that are effective against a gene of interest, the gene to be targeted is cloned into an expression vector as a translational fusion to a fluorescent protein. This construct is then co-transfected with test and control siRNA sequences against the gene. If the siRNA sequence is effective, then expression of the fusion protein will be reduced, resulting in a loss of fluorescence.

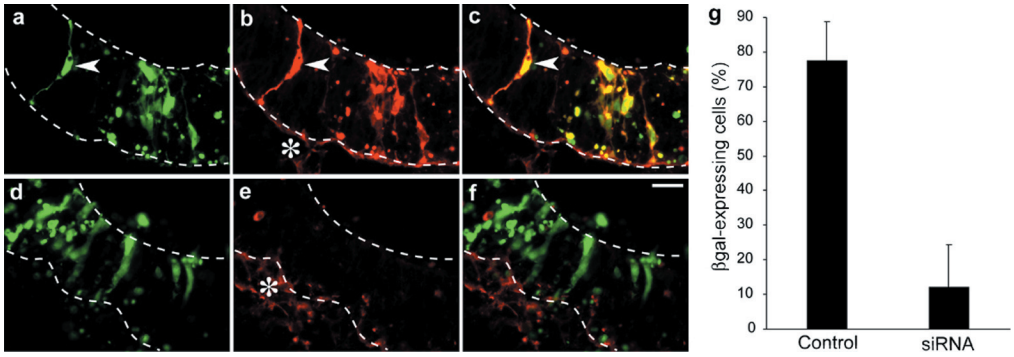

Figure 15.4. RNAi in the neuroepithelium of E10 mouse embryos. E10 mouse embryos were injected, into the lumen of the telencephalic neural tube, with the two reporter plasmids pEGFP-N2 (for GFP) and pSVpaXD (for βgal), either without (**a–c** and **g**, **Control**) or with (**d-f** and **g**, **siRNA**) βgal-directed esiRNAs, followed by directional electroporation and whole embryo culture for 24 hours. (**a-f**) Horizontal cryosections through the targeted region of the telencenphalon were analysed by double fluorescence for expression of GFP (green; **a** and **d**) and βgal immunoreactivity (red; **b** and **e**). Co-expression of GFP and βgal in neuroepithelial cells appears yellow in the merge (**c** and **f**, **arrowheads**). Note the lack of βgal expression in neuroepithelial cells in the presence of βgal-directed esiRNAs. Upper and lower dashed lines indicate the lumenal (apical) surface and basal border of the neuroepithelium, respectively. Asterisks in (**b** and **e**) indicate signal due to the cross-reaction of the secondary antibody used to detect βgal with the basal lamina and underlying mesenchymal cells. Scale bar in (**f**), 20 μm. (**g**) Quantitation of the percentage of GFP-expressing neuroepithelial cells that also express βgal without (**Control**) or with (**siRNA**) application of βgal-directed esiRNAs. Data are the mean of three embryos analyzed as in (**a-f**); bars indicate S.D. (Reprinted figure with permission from PNAS).

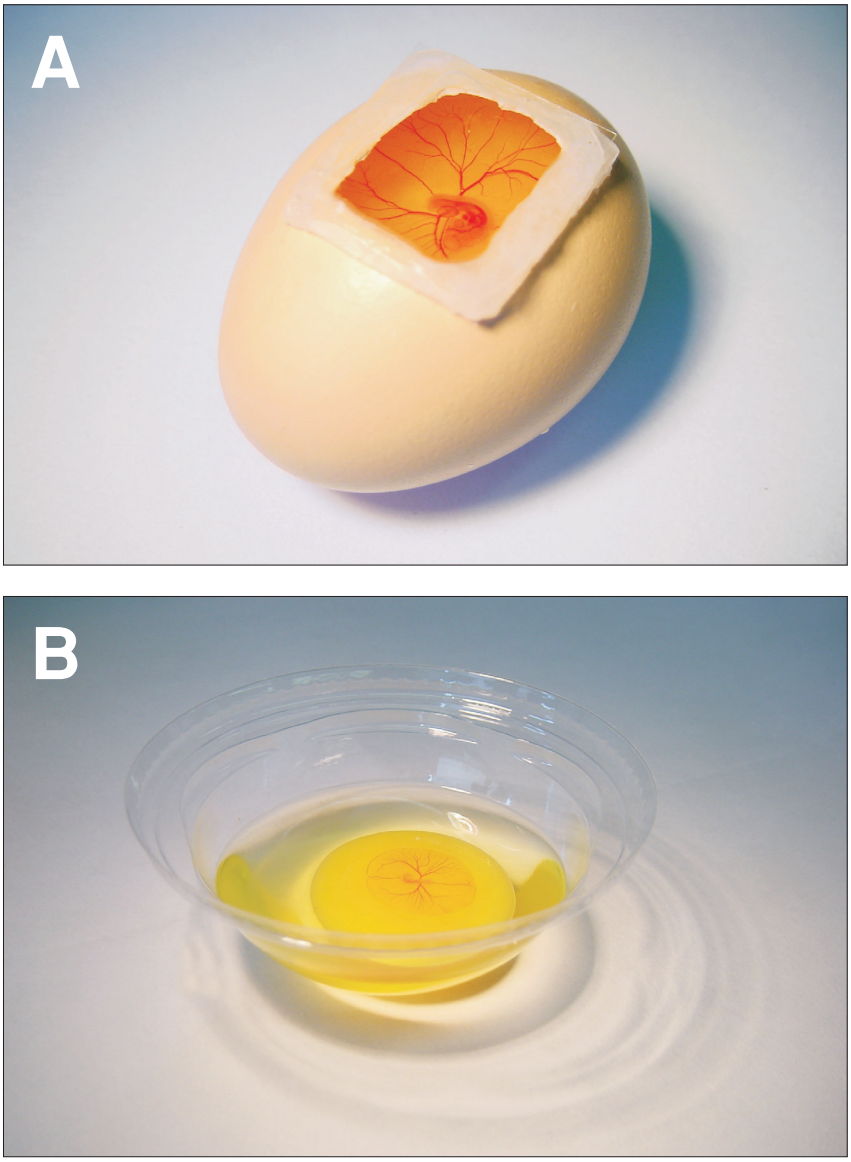

Figure 16.1. Chicken embryos are a good model system for developmental studies due to their accessibility. Chicken embryos can be accessed in ovo (A) through a window in the eggshell that can be resealed after manipulations with a coverslip and melted paraffin. As an alternative approach, chicken embryos can be used as ex ovo cultures (B). With both methods embryos can be kept alive throughout embryonic development.

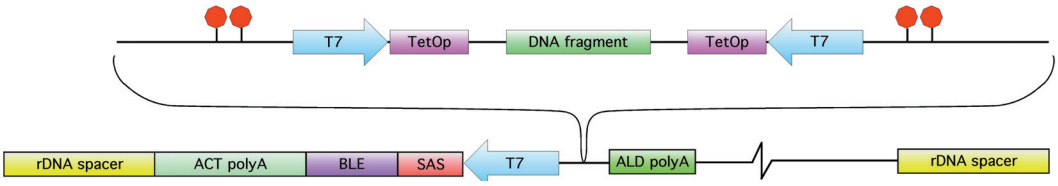

Figure 18.2. The pZJM RNAi vector. The tet operator (*Tet Op*), dual T7 terminators (red octagons), tet-inducible T7 promoters (*T7 arrows*), ribosomal DNA spacer (*rDNA*), actin poly(A) addition sequence (*ACT polyA*), phleomycin resistance gene (*BLE*), splice acceptor site (*SAS*), aldolase poly(A) addition sequence (*ALD polyA*). The plasmid is shown in linearized form, after cleavage in the rDNA spacer, and is not drawn to scale.

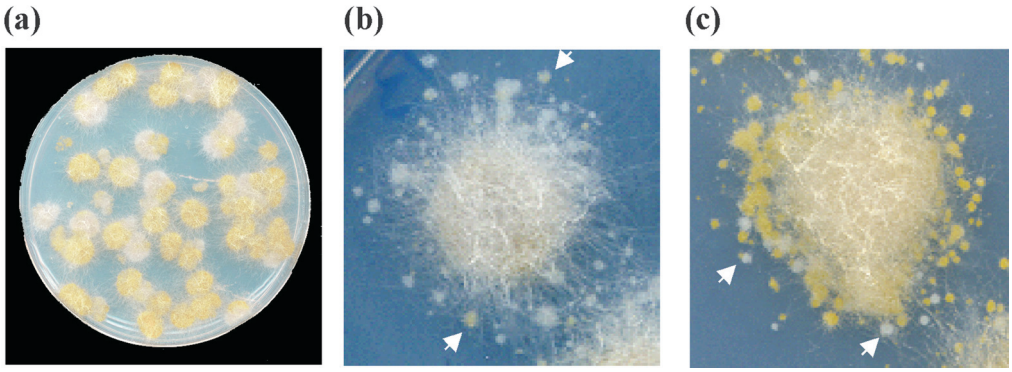

Figure 20.1. (a) Albino and wild type (yellow) colonies obtained by transformation of the wild type strain with *carB* sequences. Segregation of albino (b) and wild-type (c) transformants after a cycle of vegetative growth. Colonies showing different phenotypes (arrows) are obtained from spores of the original transformants. Photographs were taken after illumination with blue light for 24 hours.

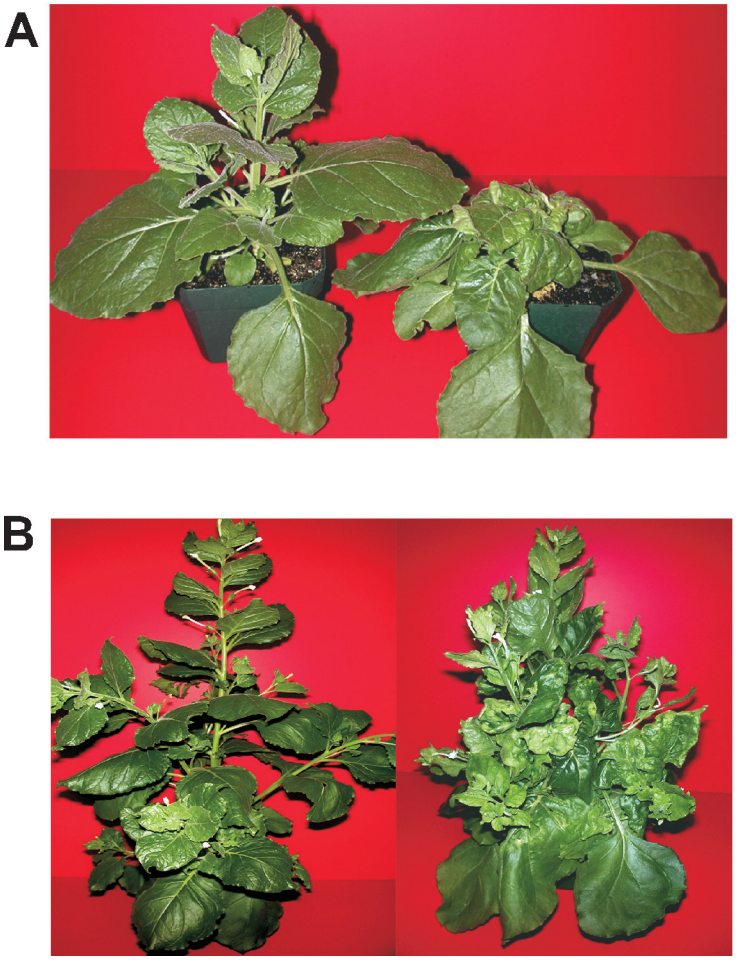

Figure 21.1. ACMV-[CM]-infected *N. benthamiana* showing recovery phenotype. *N. benthamiana* plants imaged at 2-weeks post inoculation [(WPI) (control-A-left; Infected-A-right)] and at 5-WPI (control-B-left; Infected-B-right).

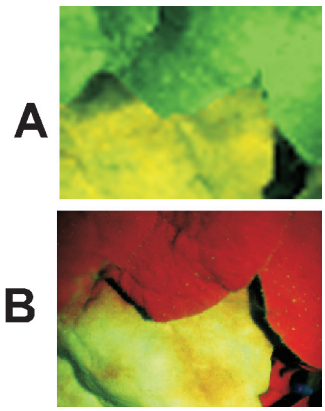

Figure 21.2. ACMV-[CM]-infected GFP silenced GFP-transgenic *N. benthamiana* (line 16C). Plant photographed using dissecting microscope (A) Normal light and (B) UV filter. Symptom-less recovered leaves appeared red under UV light.

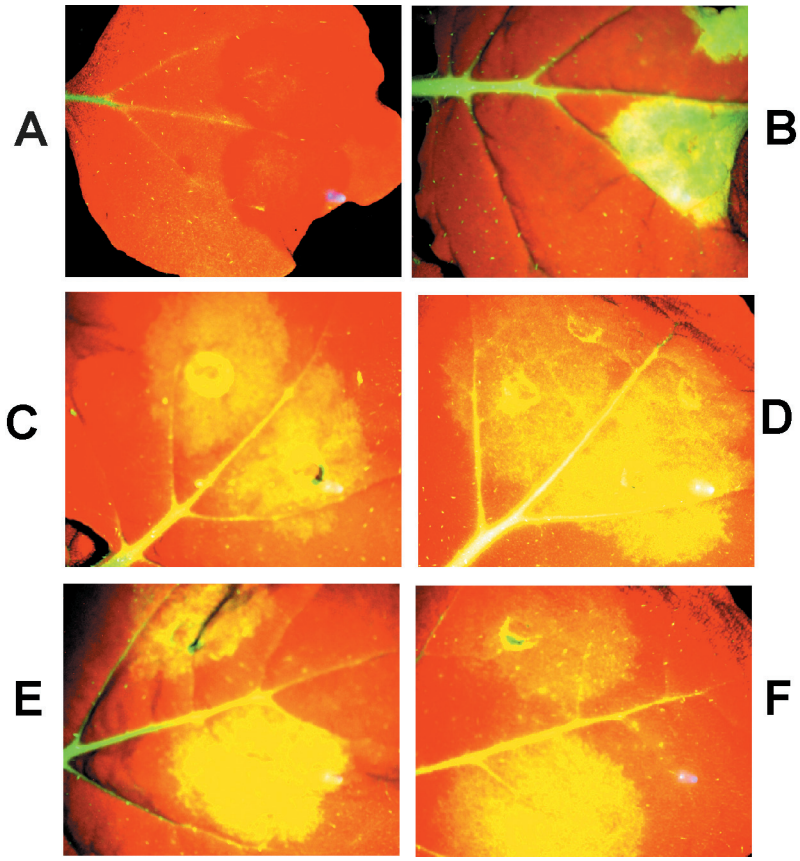

Figure 21.3. Effect of anti-PTGS activity of AC2 gene of EACMCV and ICMV; and AC4 gene of ACMV-[CM] and SLCMV. Leaf of GFP-transgenic *N. benthamiana* (line 16C) plant agroinfiltrated with pBin-GFP alone (A), or bacterial mixture harboring pBin-GFP along with the following viral gene constructs, P1/HC-Pro of TEV (B); AC4 of ACMV-[CM] (C), AC2 of EACMCV (D), AC4 of SLCMV (E) and AC2 of ICMV (F). Leaves were photographed 7 days after infiltration using a dissecting microscope.

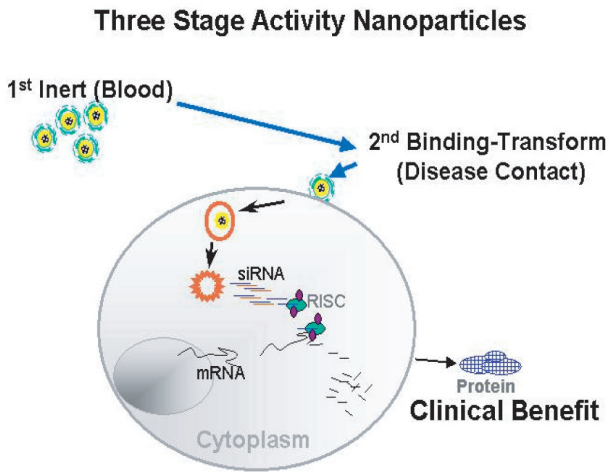

Figure 22.2. Ideal System for systemic delivery of siRNA.

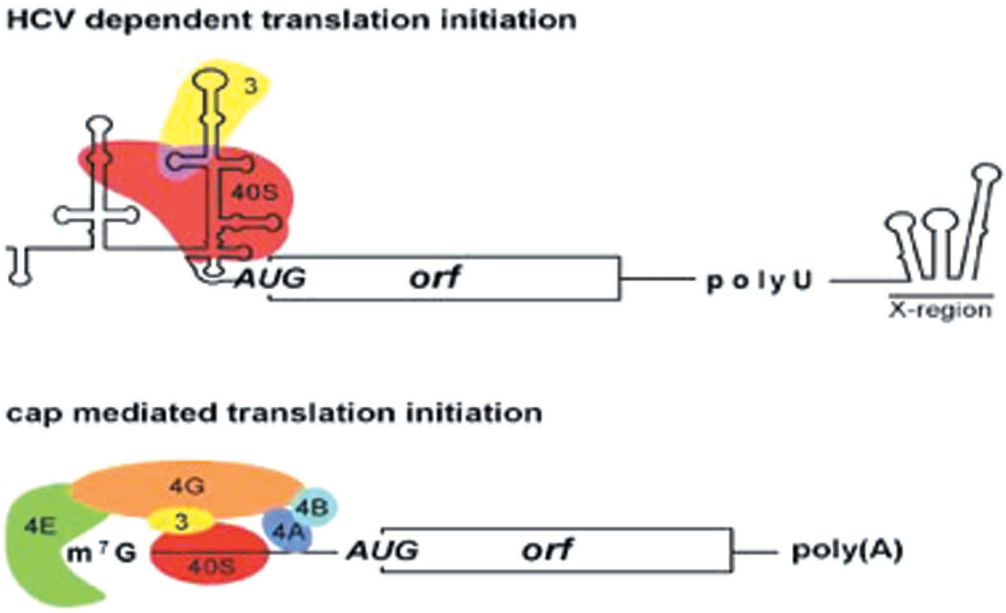

Figure 23.1. Comparison of HCV-IRES- and 5′ cap- dependent translation A) The HCV-IRES driven internal translation initiation, starts with the direct recruitment of the 40S ribosomal subunit and the eukaryotic initiation factor eIF 3. In cap-dependent translation initiation, the recruitment of the 40S ribosomal subunit requires the recognition of the m^7GpppG cap at the mRNA 5′end, by the initiation factor eIF4E at which the eIF 4F complex, consisting of the initiation factors eIF 4E, eIF 4G and eIF 4A, is assembled. The recruitment of the 40S ribosomal subunit takes place via eIF 3 which binds to eIF4G.

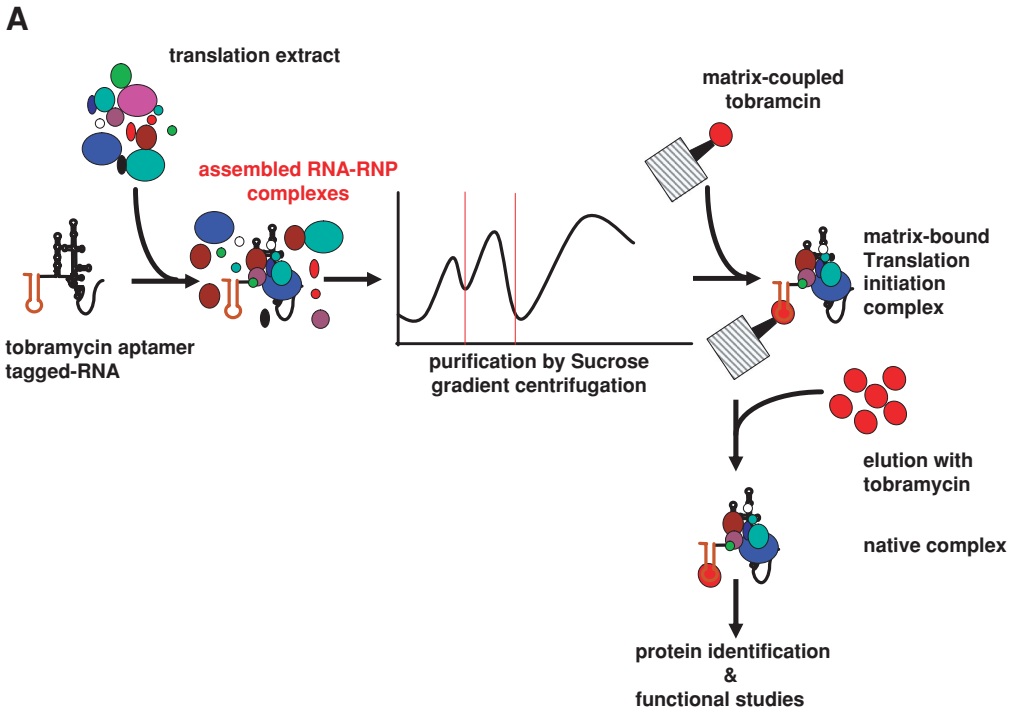

Figure 23.2. Tobramycin-tag affinity chromatography of translation initiation complex A) The HCV RNA 5′UTR bearing the HCV-IRES fused to the tobramycin aptamer was incubated with cytoplasmic HeLa cell extract under physiological conditions. Protein complexes assembled on the 5′UTR sequence were loaded on a 5–25% sucrose gradient and distributed according to their molecular weight by ultracentrifugation. The resulting 48S ribosomal peak fractions were subsequently incubated with the sepharose-coupled aminoglycoside tobramycin. Following extensive washing of the affinity matrix, proteins were eluted from the complex assembled at the HCV-IRES. Proteins eluted from the HCV-IRES were isolated from a silver stained polyacrylamide gel and identified by mass spectrometry (LC-MS) according to representative peptides.

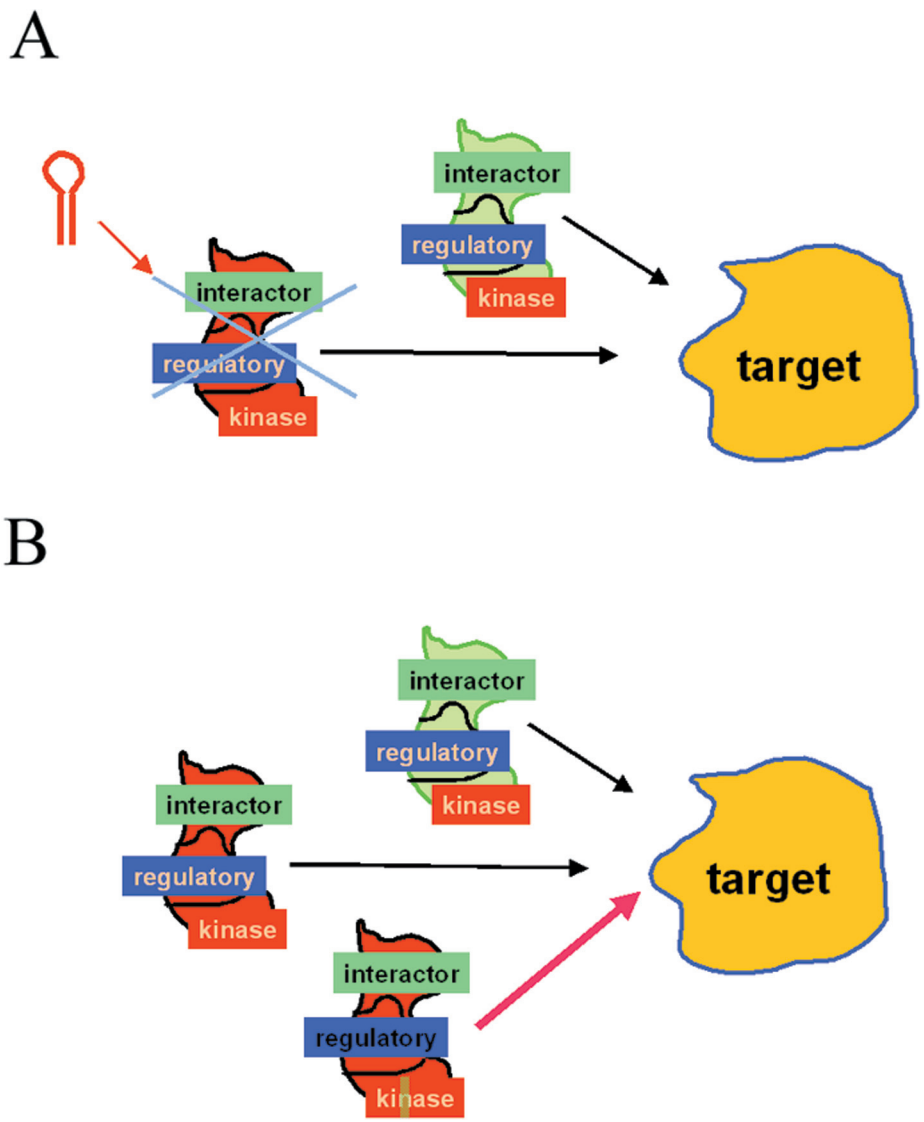

Figure 24.4. *Schematic models of interference of protein kinases by RNAi knockdown and dominant negative mutant.* Two kinases are depicted as interacting with the same target. Inhibition by RNAi or dominant negative is depicted in red in each part of the figure. A. Knockdown of a kinase by shRNA removes the targeted kinase from the cell. B. Inhibition of kinases by expression of a dominant negative mutant.

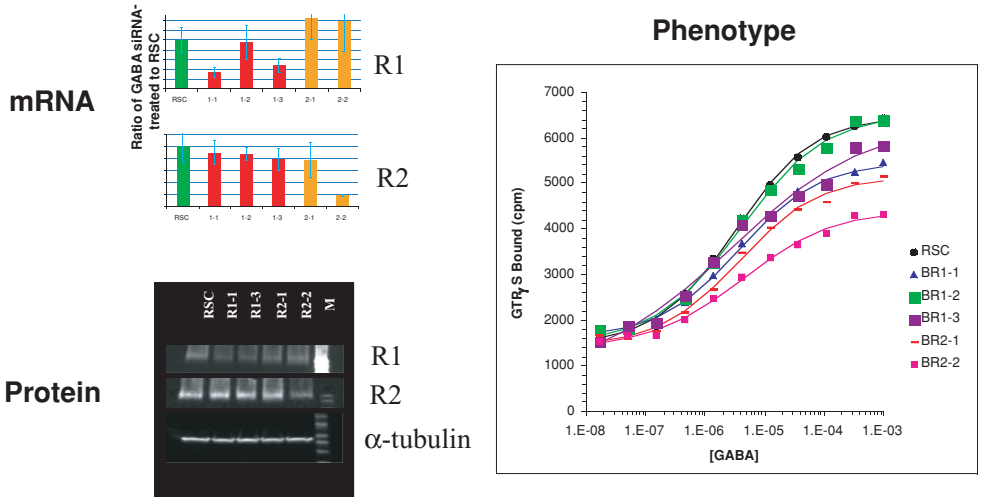

Figure 25.3. Consequences of RNAi-mediated knockdown on$GABA_BR1$ and $GABA_BR2$ receptors. mRNA levels of $GABA_BR1$ and $GABA_BR2$ were determined 24 hours post transfection with specific siRNAs. The green bar indicates the random sequence control, the red bars (1−1, 1−2 and 1−3) are siRNAs specific for $GABA_BR1$, the orange bars (2−1 and 2−2) show siRNAs specific for $GABA_BR2$. **Protein** knockdown of $GABA_BR1$ and $GABA_BR2$ was analysed after treatment of cells for 72 hours with siRNAs, and quantified by immunoblot relative to the internal control, α-tubulin. The **phenotype** associated with the knockdown of $GABA_BR1$ and $GABA_BR2$ was characterised using a ^{35}S GTPγassay.

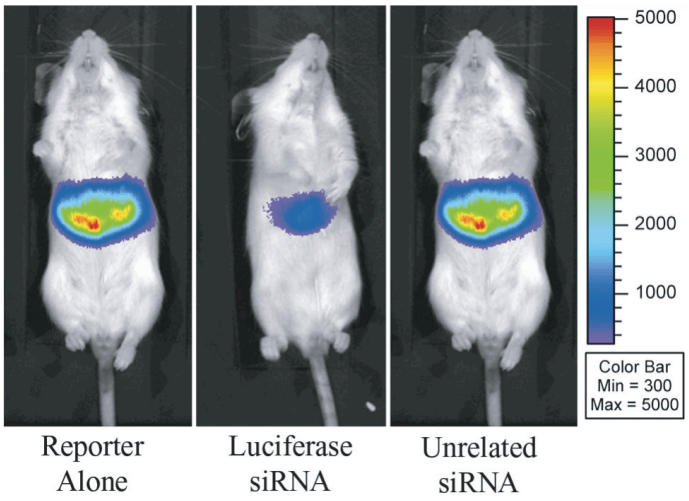

Figure 27.2. Light emitted from living mice as the result of luciferase expression is significantly reduced in the presence of luciferase siRNAs. Representative images of mice co-transfected with the luciferase plasmid pGL3-Control and either no siRNA (left), luciferase siRNA (middle) or unrelated siRNA (right). A pseudocolor image representing intensity of emitted light (red most and blue least intense) superimposed on a grayscale reference image (for orientation) shows that.RNAi functions in adult mammals. Forty μg of annealed 21-mer siRNAs (Dharmacon) were hydrodynamically transfected into livers of mice with the 2 μg of pGL3-Control DNA. Seventy two hours after transfection, mice were anesthetized and given 3 mg of luciferin intraperitoneally 15 min prior to imaging with a cooled CCD camera. IVIS imaging system (Xenogen, Alameda, CA) courtesy of Dr. Christopher Contag, Stanford University. Image reprinted with permission from McCaffrey et al., 2004.

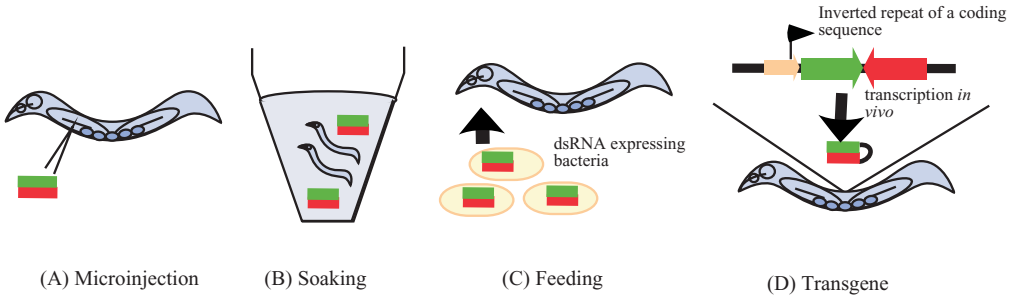

Figure 30.1. dsRNA delivery methods. (A) Microinjection of the *in vitro* synthesized dsRNA. (B) Soaking in the dsRNA solution. (C) Feeding bacteria that express dsRNA. (D) *In vivo* transcription of hairpin RNAs from the transgene. By choosing promoters that control the expression of hairpin RNAs, inducible- or tissue-specific RNAi can be elicited.

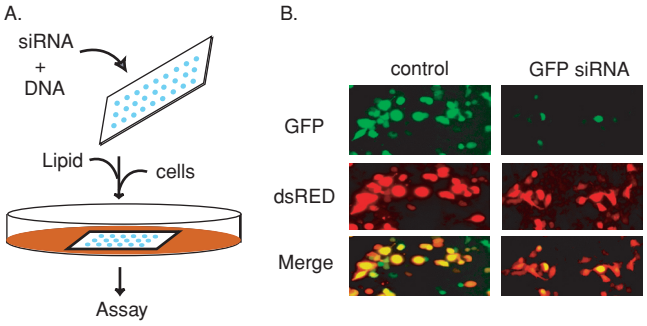

Figure 33.1. siRNA microarray for gene silencing. (A) Experimental strategy for siRNA microarrays. The desired cDNA and siRNAs are printed as individual spots on glass slides and exposed briefly to lipid before placing HEK293 cells on the printed slides in culture dish. Transfected cells are visualized using fluorescent microscopy and evaluated for the effect of RNAi. (B) Parallel RNAi on microarrays. Fluorescence photomicrograph of cells after reverse transfection of the indicated siRNA and cDNAs is shown.

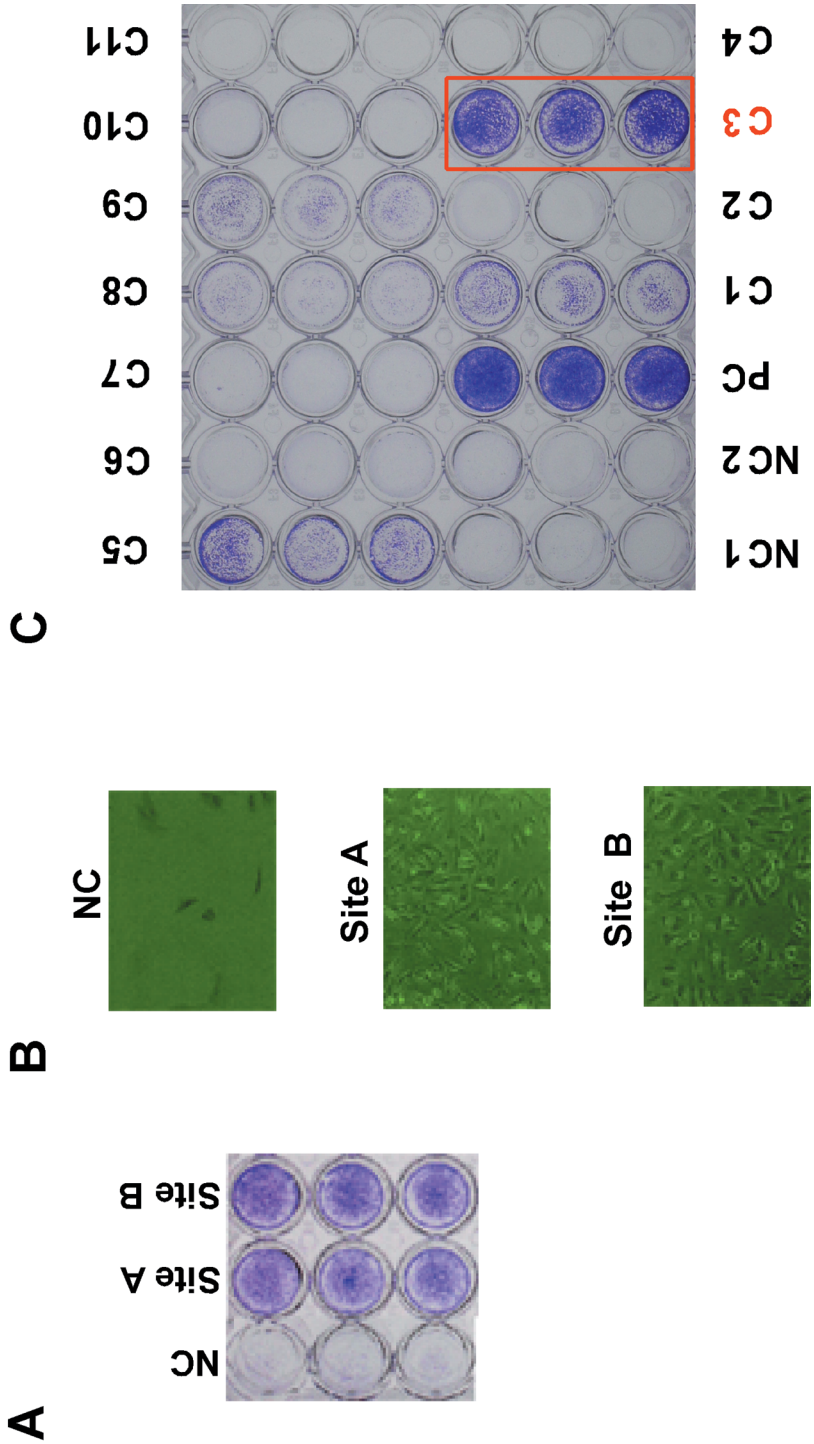

Figure 34.6. Identification of a previously unidentified gene that is involved in apoptosis in human cells. (A) shRNAi vectors directed against two sites (A and B) in the transcript of the gene for protein kinase R (PKR) prevented apoptosis in response to dsRNA. After the induction of apoptosis and fixation, HeLa S3 cells were stained with crystal violet, which only stains living cells. NC, Negative control. (B) Images of cells shown in (A) prior to staining. (C) The shRNAs designated C1 through C11 were tested for their ability to prevent apoptosis. These shRNAs were designed to target the transcripts of genes for kinases or transcription factors or genes that might be related to apoptosis. Each shRNA was tested in triplicate and cells that had been challenged with dsRNA were fixed and subjected to staining with crystal violet. PC, Positive control (shRNA directed against the gene for PKR; NC1 and NC2, negative controls; C1 through C11, shRNAs directed against specific genes. The shRNA designated C3 prevented apoptosis and the cells were stained purple with crystal violet.